Differential Dynamic Microscopy: Probing Wave Vector Dependent Dynamics with a Microscope

Roberto Cerbino[1,2,*] and Veronique Trappe[1]

[1]*Department of Physics, University of Fribourg, Chemin du Musée 3, CH-1700, Fribourg, Switzerland*
[2]*Department of Chemistry, Biochemistry and Medical Biotechnologies, Universitá degli Studi di Milano, I-20133 Milano, Italy*

We demonstrate the use of an ordinary white-light microscope for the study of the q-dependent dynamics of colloidal dispersions. Time series of digital video images are acquired in bright field with a fast camera, and image differences are Fourier analyzed as a function of the time delay between them. This allows for the characterization of the particle dynamics independent of whether or not they can be resolved individually. The characteristic times are measured in a wide range of wave vectors and the results are found to be in good agreement with the theoretically expected values for Brownian motion in a viscous medium.

Microscopy and light scattering are widely used in physics, chemistry, biology, and medical laboratories to access information on the structure and dynamics of mesoscopic systems. While microscopy gives direct access to real space images, scattering techniques work in reciprocal space, where information on the structure and dynamics of the system is obtained, respectively, from the angular and time dependence of the scattered light intensity [1]. These two complementary techniques have in general very different experimental requirements. White-light sources are usual choices in microscopy, while a certain degree of coherence of the illuminating beam is required in scattering experiments; this is usually achieved by using a laser. In the past many attempts have been made to build a scattering apparatus based on a microscope; all of these attempts involved the use of a laser as an illumination source (see, for example, Refs. [2–6], and references therein). In some cases special care was taken to ensure the capability to perform microscopy and scattering experiments simultaneously, thereby allowing for a powerful combination of the complementary information obtained by both techniques [2,3]. More recently, microscope-based laser dynamic light scattering (DLS) experiments have been developed to study the dynamic properties of samples of biological interest, such as living macrophage and red blood cells [5,6]. In practice, because of the intrinsic difficulties in building such instruments, the use of such techniques has been restricted to those laboratories, where a sufficient expertise in the realization of optical instrumentation was at hand.

In this Letter, we present a conceptual scheme to interpret and analyze microscopy images that are obtained from samples containing moving entities. This technique, which we term differential dynamic microscopy (DDM), does not entail any special experimental requirements, being based on the use of a standard light microscope with a normal illumination source and a digital video camera. By using the tools of Fourier optics [7] we provide the means to access information about the sample dynamics that are equivalent to the one obtained in multiangle DLS experiments [8]. We test DDM by analyzing time sequences of microscopy images obtained with an aqueous dispersion of colloidal particles with diameter 73 nm, well below the resolution limit of the microscope. Additional tests are performed with larger particles (diameter 420 nm). Our results are in good agreement with the predictions from the theory of Brownian motion in a viscous medium, thereby validating the proposed analysis. We believe that DDM is an interesting complement to the well established DLS [9] and microscope video tracking [10] techniques.

Our experimental setup simply consists of an inverted microscope (LEICA DM IRB) equipped with a complementary metal-oxide-semiconductor (CMOS) camera (IDT X-Stream XS-3, 1280×1024 pixels, pixel size = $12 \ \mu$m). No modifications are made to the microscope. The sample is illuminated by focusing white light on the sample with a condenser lens (numerical aperture 0.9); for detection we use a standard objective (magnification $M = 63 \times$, numerical aperture NA = 0.7). The effective pixel size, accounting for the magnification M, is then given by $d_{pix} = 0.19 \ \mu$m, a value smaller than the microscope resolution limit imposed by diffraction. A capillary tube with a rectangular section (Vitrocom, Inc.) is filled with an aqueous dispersion of polystyrene spheres of diameter 73 nm (Duke Scientific, part no. 3070 A). The concentration is 1% by weight fraction, sufficiently low to neglect the effect of interactions between individual spheres. The thickness of the capillary tube along the microscope optical axis is 100 μm and a region at the center of the capillary tube is imaged onto the camera sensor.

A sequence of $N = 1000$ images is acquired with a sampling rate of 100 samples/s and with an exposure time of 1 ms. In Fig. 1(a) we show a typical image: the image appears as a bright background with some dark spots. These dark spots are dust particles located mainly on the protective glass of the camera sensor. The signal due to the particles is barely visible as its contribution is small compared to the large background signal. However, the
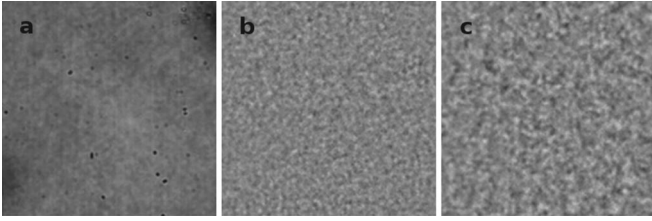
P H Y S I C A L   R E V I E W   L E T T E R S

FIG. 1. (a) Microscope image of an aqueous dispersion of 73 nm particles at a weight fraction of 1%. The particles are below the resolution of the microscope and the signal generated by them is very small. (b) Result of the subtraction of two images taken 10 ms apart in time. The signal due to the particles is now visible. (c) Result of the subtraction of two images 200 ms apart in time. The signal has increased. The size of each panel corresponds to 47 μm in the sample.

background is a static contribution, while the Brownian motion of the particles causes an incessant rearrangement of their configuration in space. By subtracting two images grabbed at different times, we can eliminate the static contributions in our image and bring the displaced particles to light. Examples of difference images obtained by this subtraction procedure are shown in Figs. 1(b) and 1(c); 1(b) and 1(c) are, respectively, the difference images obtained by subtracting two images separated in time by $\Delta t = 10$ ms and $\Delta t = 200$ ms. Clearly, the grainy appearance of the difference images increases with increasing time delay Δt, revealing the increasing displacement of the particles.

We can quantify this increase by calculating the spatial variance,

$$\sigma^2(\Delta t) = \int |D(x, y; \Delta t)|^2 dxdy, \qquad (1)$$

of the difference signal $D(x, y; \Delta t) = I(x, y; \Delta t) - I(x, y; 0)$ as a function of Δt. Here, $I(x, y; t)$ is the intensity obtained in the sensor plane (x, y) at the time t, where we define the acquisition time of the first image to be $t = 0$ s. The actual choice of the reference image is not crucial in the case of Brownian motion, since the statistical properties of the investigated dynamics do not change in time. This can be appreciated in the movie clips shown in [11], where the time delay between two subtracted images is kept constant at $\Delta t = 200$ ms. Consequently, for every Δt we calculate the variance $\sigma^2(\Delta t)$ by averaging over many statistical realizations of the signal, typically 100, to improve the statistical accuracy. As shown in Fig. 2, the variance $\sigma^2(\Delta t)$, increases very rapidly with Δt and attains a steady state plateau at long times, when all the particles have moved far away from their initial position, such that the two images used to obtain the difference image are statistically uncorrelated. This dependence of the variance on Δt clearly indicates that difference images can be used to monitor the particle dynamics. The question then arises whether it is possible to extract quantitative information on
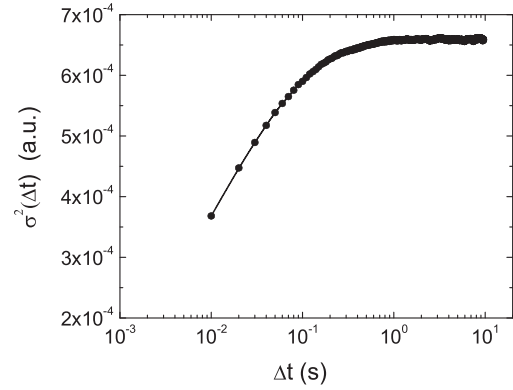

FIG. 2. The particles rearrangement due to their Brownian motion causes an increase of the variance $\sigma^2(\Delta t)$ of the difference signal $D(x, y; \Delta t)$. With increasing time delay the two subtracted images become progressively uncorrelated, such that $\sigma^2(\Delta t)$ saturates at large Δt.

the dynamics of the system from the difference images. The answer is yes, but its justification requires the use of two steps.

The first one is to consider that the variance, defined in Eq. (1), can be calculated in the Fourier space as well. If we define the 2D Fourier transform of $D(x, y; \Delta t)$ as $F_D(u_x, u_y; \Delta t) = \int D(x, y; \Delta t) \exp[-i2\pi(u_x x + u_y y)]dxdy$, the use of the Parseval theorem [7] guarantees that

$$\sigma^2(\Delta t) = \int |F_D(u_x, u_y; \Delta t)|^2 du_x du_y. \qquad (2)$$

The equivalence of Eq. (1) and (2) shows that the total energy content of D in real space is the same as the one of F_D in Fourier space. However, in Fourier space it is possible to isolate every Fourier component and study the growth of its amplitude as a function of Δt.

To clarify whether this mode decomposition provides insight about the dynamics of the system, we need to go through the second step. This step consists in realizing that a Fourier component of the microscope image is associated in a simple way with a scattering angle and in turn with a scattering wave vector. According to Abbe's theory of microscope image formation [7,12], the object to be imaged on the camera sensor can be thought of as the superposition of different Fourier components characterized by a spatial frequency u_{obj}. Each frequency component of the object acts as a grating and diffracts light at an angle $\vartheta = \sin^{-1}(\lambda u_{obj})$ with respect to the microscope optical axis, where λ is the wavelength of light. On the camera sensor, the diffracted plane wave will produce a sinusoidal fringe pattern, characterized by a spatial frequency $u_{det} = \sin(\vartheta)/\lambda = u_{obj}$, independent of the wavelength λ. This guarantees that we can associate, in a unique way, a spatial frequency u_{det} on the detector to a scattering angle ϑ.

To investigate the angular dependent dynamics of our system, we thus use the Fourier power spectrum

$|F_D(u_x, u_y; \Delta t)|^2$, which we simply calculate by applying a fast Fourier transform [13] to the difference images. For isotropic samples, like the one investigated, the expectation value of $|F_D(u_x, u_y; \Delta t)|^2$ is rotationally invariant in the (u_x, u_y) plane. This allows us to perform azimuthal averages and to treat the one-dimensional power spectrum $|F_D(u; \Delta t)|^2$, where $u = \sqrt{u_x^2 + u_y^2}$. For easy comparison with scattering experiments we use wave vectors $q = 2\pi u$ instead of spatial frequencies u. Processing the data at several Δt enables us to report the one-dimensional power spectrum $|F_D(q; \Delta t)|^2$ as a function of the time delay, as shown for three values of q ($q = 2.6\ \mu\text{m}^{-1}$, $q = 3.9\ \mu\text{m}^{-1}$, and $q = 4.5\ \mu\text{m}^{-1}$) in Fig. 3. As for the variance $\sigma^2(\Delta t)$ we find that $|F_D(q; \Delta t)|^2$ increases rapidly with Δt to then saturate at longer time delays. The crossover to the plateau value systematically shifts to smaller Δt as the wave vector q increases, denoting a q dependence in the characteristic time of the system.

For a quantitative description of this behavior we consider that fluctuations in the intensity of the original images are due to concentration fluctuations in the sample. For Brownian diffusion it is well known that every Fourier concentration mode decays exponentially in time, $\exp(-\Delta t/\tau(q))$, with a characteristic time $\tau(q) = 1/D_m q^2$, where D_m is the mass diffusion coefficient of the particles [9]. For the analysis of the difference images it is then easy to show that

$$|F_D(q; \Delta t)|^2 = A(q)[1 - \exp(-\Delta t/\tau(q))] + B(q). \quad (3)$$

This equation contains two main contributions: the term $B(q)$ is due to the power spectrum of the camera noise and is present even in the absence of the particles. The term $A(q)[1 - \exp(-\Delta t/\tau(q))]$ describes the contribution associated with the particles. A quantitative description of the term $A(q)$ requires the knowledge of the exact relationship between intensity and concentration fluctuations, which is beyond the scope of this Letter. However, once
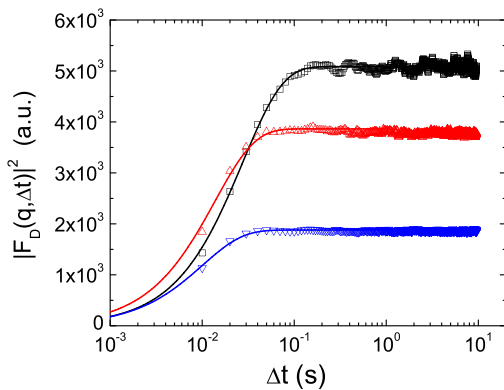
q is fixed, we can treat $A(q)$ and $B(q)$ as simple adjusting parameters and extract the characteristic time $\tau(q)$ by simply considering the Δt dependence of $|F_D(q; \Delta t)|^2$. This is very similar to what has been done in Ref. [14] where an expression similar to Eq. (3) has been proposed to analyze sequences of shadowgraph images for the characterization of nonequilibrium concentration fluctuations in a binary mixture.

Thus, we fit our data to Eq. (3) to obtain $\tau(q)$, which we report in Fig. 4 for q ranging from 0.4 μm^{-1} to 5 μm^{-1} (black open circles). On the same graph the dotted black line denotes the expected behavior calculated by using the formula $\tau(q) = 1/D_m q^2$, where D_m is estimated using the Stokes-Einstein relation $D_m = k_B T/(3\pi\eta d) = 5.98\ \mu\text{m}^2/\text{s}$; k_B is the Boltzmann constant, T the absolute temperature, η the solvent viscosity, and d the diameter of the particles. The experimental results are in good agreement with the theoretically expected values over more than one decade in q, showing that DDM is a reliable means to determine the dynamical properties of the sample. To our knowledge, this result provides the first experimental evidence that white-light, bright-field microscopy can be used to monitor the q-dependent dynamics of particles.

We also perform experiments by using particles with a diameter of 420 nm, value comparable to the point spread function of the microscope. In Fig. 5 we present two images of this sample separated in time by 10 s. In contrast to the previous case, the particles are fairly visible, though the static signal due to dust along the optical path still represents a significant contribution. However, the subtraction procedure described above can still be applied to visualize the particles' motion and to eliminate the static noise, as shown in the movie clip referred to in [11]. The image sequence is analyzed as described above and the results are presented in Fig. 4 as blue open squares. A good
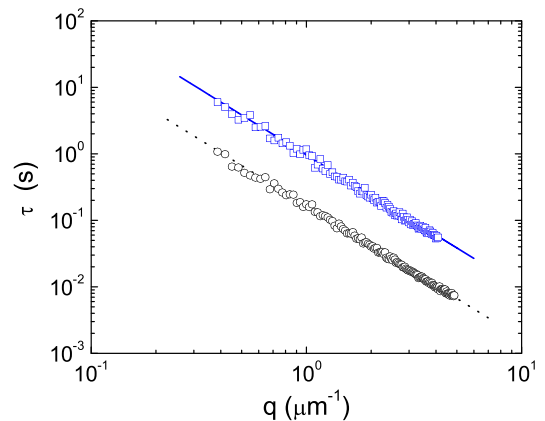
FIG. 3 (color online). Growth of $|F_D(q; \Delta t)|^2$ with Δt for three values of q: $q = 2.6\ \mu\text{m}^{-1}$ (black squares), $q = 3.9\ \mu\text{m}^{-1}$ (red up-triangles), and $q = 4.5\ \mu\text{m}^{-1}$ (blue down-triangles). The continuous lines are fits of the data to Eq. (3).

FIG. 4 (color online). Characteristic decay time τ versus the wave vector q for the 73 nm (black circles) and the 420 nm (blue squares) particles. Fitting of the data gives, respectively, the values $D_m = 6.2 \pm 0.3\ \mu\text{m}^2/\text{s}$ and $D_m = 1.1 \pm 0.2\ \mu\text{m}^2/\text{s}$. The lines are theoretical predictions calculated by using the Stokes-Einstein relation with no adjustable parameters.
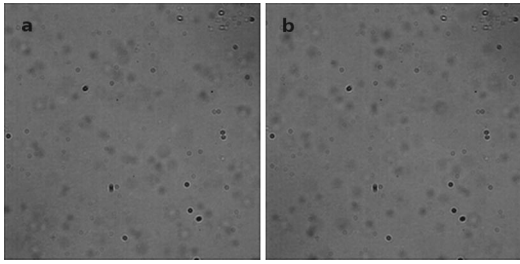
FIG. 5.   Microscope images taken 10 s apart. The side of each panel corresponds to 47 μm in the sample. The sample is a colloidal dispersion of 420 nm particles. The more visible objects are dust particles on the CMOS sensor, which are also present in Fig. 1(a), grabbed with another sample. The particles are the less visible objects that change position between image (a) and image (b). The smearing effect due to the finite point spread function of the microscope is visible.

agreement with the theoretically expected behavior ($D_m = 1.04$ μm^2/s, continuous blue line) is also found in this case, demonstrating that DDM is capable of monitoring the dynamics of particles that can either be resolved individually or not. This suggests that DDM could be a valid complement to tracking techniques [10] for relatively big particles, with the advantage of also being applicable to concentrated systems, where tracking becomes difficult, and to fluctuating systems, which are not composed by particles. Typical examples are membranes, interfaces, or liquid crystals. For small particles DDM can be subsidiary to DLS experiments [9], because it can operate at small wave vectors where stray light makes the use of DLS notoriously difficult. The range of accessible time scales is limited by the inverse of the acquisition frame rate on the lower side and by the overall duration of the experiment on the higher end.

A possible extension of this work could be the investigation of dynamically heterogeneous systems, where a space resolved investigation of the dynamics is of fundamental importance [15]. Our technique could also be applied to absorbing samples and to fluorescence microscopy, which is widely used for the investigation of biological samples [16]. Finally, we believe that DDM can be profitably used to perform microrheology experiments as pioneered in Ref. [17].

 *roberto.cerbino@unimi.it
 [1] B. Chu, *Laser Light Scattering: Basic Principles and Practice* (Dover, New York, 2007), 2nd ed.
 [2] P. D. Kaplan, V. Trappe, and D. A. Weitz, Appl. Opt. **38**, 4151 (1999).
 [3] M. T. Valentine, A. K. Popp, P. D. Kaplan, and D. A. Weitz, Opt. Lett. **26**, 890 (2001).
 [4] R. Dzakpasu and D. Axelrod, Biophys. J. **87**, 1279 (2004).
 [5] R. Dzakpasu and D. Axelrod, Biophys. J. **87**, 1288 (2004).
 [6] M. S. Amin, Y. Park, N. Lue, R. R. Dasari, K. Badizadegan, M. S. Feld, and G. Popescu, Opt. Express **15**, 17001 (2007).
 [7] J. W. Goodman, *Introduction to Fourier Optics* (Roberts & Company, Englewood, 2005), 3rd ed.
 [8] L. Cipelletti and D. A. Weitz, Rev. Sci. Instrum. **70**, 3214 (1999).
 [9] B. J. Berne and R. Pecora, *Dynamic Light Scattering: With Applications to Chemistry, Biology, and Physics* (Dover, New York, 2000).
[10] J. C. Crocker and D. G. Grier, J. Colloid Interface Sci. **179**, 298 (1996).
[11] See EPAPS Document No. E-PRLTAO-100-052819 for movie clips comparing the time evolution of microscopy images versus differences of images separated in time by a fixed time delay. For more information on EPAPS, see http://www.aip.org/pubservs/epaps.html.
[12] H. Kohler, Opt. Acta **28**, 1691 (1981).
[13] R. N. Bracewell, *The Fourier Transform and Its Application* (McGraw-Hill, New York, 1999), 3rd ed.
[14] F. Croccolo, D. Brogioli, A. Vailati, M. Giglio, and D. S. Cannell, Ann. N.Y. Acad. Sci. **1077**, 365 (2006).
[15] L. Cipelletti and L. Ramos, J. Phys. Condens. Matter **17**, R253 (2005).
[16] J. W. Lichtman and J. A. Conchello, Nat. Methods **2**, 910 (2005).
[17] T. G. Mason and D. A. Weitz, Phys. Rev. Lett. **74**, 1250 (1995).